Reduction of Pyruvate by Titanium(III)

J. KONSTANTATOS, E. VRACHNOU-ASTRA*

Department of Chemistry, Nuclear Research Center "Demokritos", Aghia Paraskevi, Attikis, Greece

and D. KATAKIS

Laboratory of Inorganic Chemistry, University of Athens, Navarinou 13A, Athens, Greece

Received August 31, 1983

Titanium(III) in aqueous solutions reacts with carbonate-like pyruvic acid and/or pyruvate to give a product of reductive coupling. The reaction was investigated kinetically over a range of hydrogen ion concentrations from 0.007 M to 2.5 M and over a wide range of concentrations of the other reactants. Under all conditions only one path was identified, corresponding to a second order rate law in $\{Ti^{III}\}$, *first order in* $\{Pyr\}$, *and inverse second order in* $\{H^+\}$.

The data are interpreted by postulating the formation of an η^2 *precursor complex between* Ti^{III} *and the carbonyl group.*

Introduction

Understanding how carbon dioxide interacts with metal ion centers, to be transformed into C–C and C–H bond containing compounds, is one of the 'paradigms' of present day chemistry. One of the approaches, pursued actively by Floriani and coworkers [1], is to simulate carbon dioxide with other double bond containing compounds. The expectation seems to be that in these models some features of the mechanism will become more prominent and easier to detect.

Along the simulation line:

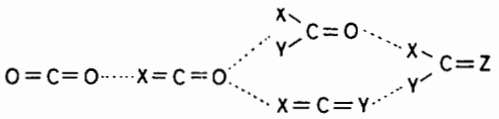

X, Y, Z ≠ oxygen atom

ketones lie closer to the end. After reducing their carbonyl group, the molecule is not CO_2-like any more. The study of the ways ketones interact with reducing metal ions provides information on the last stages in CO_2 fixation.

*Author to whom correspondence should be addressed.

The results with low-valent group VIII metal ions [2] show that the fragment L_nM containing the metal ion adds to the carbonyl bond and reacts further to give chelated complexes with dimers of the type:

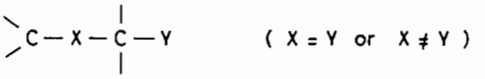

bound to the metal through the first C and Y. Dimers of the type:

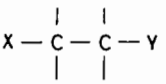

1

were not observed. In contrast, reductive coupling giving *1* can be achieved using early transition metals [1], notably $CpTiCl_2$ and $Cp_2Ti(CO)_2$.

On the other hand, it has been known for more than fifty years [3] that reductive coupling of some ketones can be achieved even in aqueous solutions, using water-soluble low-valent metal ions. Isolation from these solutions of intermediates with metal-carbon bonds is generally difficult. As a result, important clues for identifying the reaction pathways are missing. Some organometallic compounds are however inert enough in aqueous solutions and have been characterized [4]. Moreover, if one is willing to rely more on the kinetics, which are directly related to the dynamic development of the system and less on the unambiguous 'still pictures' provided by stable intermediates, water chemistry is very convenient and it broadens the scope of the efforts made, by using metal ions or complexes and unsaturated compounds inaccessible in non-aqueous solvents. In addition, we should not underestimate the practical value of using a cheap, readily available solvent.

The CO_2-like compound used in the present work is pyruvic acid and resembles the form CO_2 takes in neutral and alkaline solutions, namely carbonate,

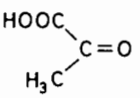

0020-1693/84/$3.00

$O\diagdown C=O^{2-}$. In this respect it should be characterized as carbonate-like. Pyruvic acid is also interesting from a biological point of view.

The reductant is Ti_{aq}^{3+}. Comparative studies with other metal ions are also available.

Experimental

Aqueous hydrochloric acid titanium(III) solutions were prepared by dissolving spectrographically-standardized titanium sponge [6] in concentrated hydrochloric acid under continuous bubbling with argon at *ca.* 70 °C. The resulting concentrated solution was diluted with triply distilled water. Sodium pyruvate (Merck) was stored at 0 °C.

The reaction takes place under air-free conditions and its progress was assessed by following the disappearance of Ti^{III} spectrophotometrically. Average absorptivities $\bar{\epsilon}$ of Ti^{III} at various pyruvic acid and hydrogen ion concentrations were obtained from zero-time absorbances (Fig. 1). In the course of a run these concentrations did not change appreciably, because all kinetic experiments were performed in excess pyruvic acid and in excess hydrogen ion or at constant pH sustained by the buffering action of the pyruvic acid-pyruvate system.

At high hydrochloric acid concentrations the reaction was followed spectrophotometrically using a Cary 14 spectrophotometer, at lower acid concentrations, where the rates are faster, using a stopped-flow apparatus (Applied Photophysics, Ltd.). The products were also examined by proton NMR, IR, and polarographically.

The overall stoichiometry of the reaction was found by determining the unreacted Ti^{III} polarographically and spectrophotometrically, and, at hydrogen ion concentrations higher than 0.5 *M*, the unreacted pyruvic acid polarographically. At 0.7 *M* HCl and 24 °C $E_{1/2}$ for pyruvic *vs.* a saturated Ag/AgCl electrode ($E^0 = 0.2$ V) is −0.64 V. pH values >0.3 were measured with a pH meter. pH values smaller than 0.3 were estimated from the acid added.

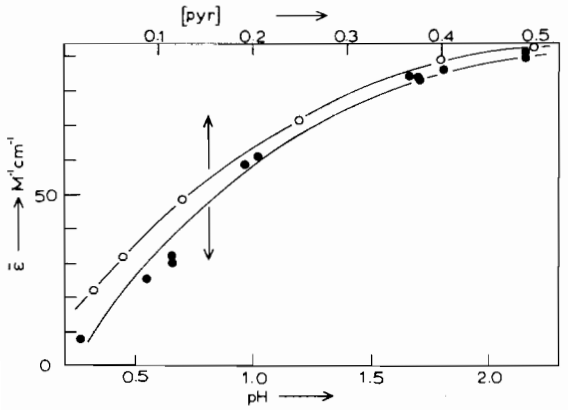

Fig. 1. Average absorptivities, $\bar{\epsilon}$, at 504 nm of Ti^{3+} are plotted: a) *versus* pH (lower curve, full circles) at [pyr] = 0.50 *M*, $[Ti^{3+}] = 0.005$ *M*, and 24 °C. b) *versus* total pyruvic acid concentration (upper curve, open circles) at $[Ti^{3+}] = 0.004$ *M*, pH = 1.72 and 24 °C.

Results

Three distinct stages were observed.

The first is a complex formation step, too fast to be followed by the stopped-flow method. This complex (complexes) has an increased absorptivity compared to Ti_{aq}^{3+} and the absorption maximum is shifted towards larger wavelengths (520 nm, Fig. 2). The shoulder in this figure is real and indicates the presence of chloride-complexed and uncomplexed species. Polarographically, however, only one anodic wave is observed, displaced towards more negative $E_{1/2}$ values as the concentration of the acid decreases (*e.g.* $E_{1/2} = -180$ V at $\{HCl\} = 0.5$ *M* and $E_{1/2} = -0.248$ V at $\{HCl\} = 0.03$ *M*, presumably because hydrolyzed Ti_{aq}^{III} is a better reductant.

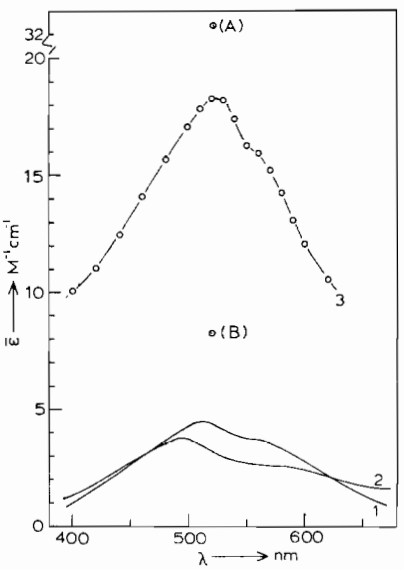

Fig. 2. Spectra of Ti^{3+}: curve (3) corresponds to the spectrum of Ti^{3+} at the following conditions: $[Ti^{3+}] = 0.022$ *M*, [pyr] = 0.50 *M*, and [HCl] = 0.55 *M*. This spectrum was obtained by the stopped-flow instrument and by extrapolating the kinetic curves, obtained every 10 nm, to zero time. Points (A) and (B) were obtained similarly, but at different hydrochloric acid and pyruvic acid concentrations. For point (A) [pyr] = 0.50 *M* and [HCl] = 0.25 *M*. For point (B) [pyr] = 0.25 *M* and [HCl] = 0.55 *M*. Curves (1) and (2) correspond to the spectra of Ti^{3+} in the absence of pyruvic acid and at HCl concentrations 1.00 and 0.01 *M* respectively. These two spectra were obtained on a conventional spectrophotometer (Cary 14) and they are shown here for comparison.

The second stage of the reaction is slower and includes the electron transfer step. This is the stage that we followed kinetically (*vide infra*).

The third stage is the slowest and is probably a condensation of the Ti^{IV} product, as indicated by the slow increase in absorbance in the uv region. The organic product is apparently contained in the Ti^{IV} polymeric species. In concentrated solutions the condensed Ti^{IV} product precipitates as a white amorphous solid of colloidal form, difficult to filter out. The proton NMR of this solid and of the reaction mixtures obtained after complete oxidation of the paramagnetic Ti^{III} gave peaks attributable to dimethyltartaric acid or unreacted pyruvic acid attached to Ti^{IV}. Peaks characteristic of lactic acid are not observed.

The overall stoichiometry of the reaction was determined both in excess pyruvic acid and excess Ti^{III}, and at various hydrogen ion concentrations. In all cases it was found to be 1:1.

The kinetic experiments using the Cary spectrophotometer and the stopped-flow apparatus are summarized in Tables I and II. Typical pseudo-second-order plots for the disappearance of Ti^{III} at various concentrations of pyruvic acid are shown in Fig. 3. Fig. 4 depicts the pseudo-second-order rate constant $k_{obs}^{(2)}$ as a function of the concentration of pyruvic acid. From these two figures it is seen that the redox reaction fits second-order kinetics very well for Ti^{III} and first order for pyruvic acid. This rate law is mostly based on data in excess pyruvic acid, but it was also verified by a few runs in excess Ti^{III}.

Chloride ion has no effect on the rate. Also, under the conditions of our experiments the rate is not affected by a change in ionic stength. However, it depends inversely on the concentration of hydrogen ions. No acid-independent term was found. It is interesting to note in this connection that the rate law for the reduction of pyruvic acid by Eu_{aq}^{2+} contains a term proportional (not inverse) to the con-

TABLE I. Kinetic Data for the Reaction Ti(III) and Pyruvic Acid Obtained by Stopped-Flow Spectrophotometry (High pH Region).

Temp. °C	$\{Ti^{3+}\}_o$ *M*	pH	$\{PYR\}_{total}$	$\bar{\epsilon}$ M^{-1} cm^{-1}	Slope*(s^{-1})	k_{obs} s^{-1} M^{-2}
32	0.01	2.00	0.500	90.0	53.9 ± 0.5	19404
32	0.01	2.00	0.500	92.0	49.1 ± 1.3	18069
32	0.01	1.82	0.350	79.0	31.1 ± 0.7	14039
32	0.01	1.78	0.250	69.0	27.5 ± 0.4	15124
32	0.01	1.74	0.200	58.0	16.6 ± 0.3	9628
32	0.01	1.70	0.125	45.0	9.3 ± 0.2	6696
32	0.01	1.46	0.062	23.0	4.0 ± 0.05	2967
30	0.01	0.64	1.00	52	0.45 ± 0.01	46.8
30	0.01	0.36	1.00	41.0	0.18 ± 0.01	14.8
30	0.01	0.33	0.50	21.5	0.17 ± 0.005	14.6
30	0.01	0.57	0.50	34.0	0.35 ± 0.005	47.6
27	0.0063	1.34	0.50	56	3.28 ± 0.05	734.7
27	0.0063	1.04	0.250	27.2	0.76 ± 0.03	165.4
27	0.0063	1.46	0.250	41.6	3.6 ± 0.07	1198
29	0.005	1.26	0.500	58.8	2.5 ± 0.08	588
29	0.005	0.80	0.500	38.8	0.43 ± 0.007	67
29	0.005	0.55	0.500	25.8	0.28 ± 0.01	28.9
29	0.005	0.27	0.500	18.2	0.035 ± 0.001	2.55
29	0.005	1.35	0.500	71.5	2.72 ± 0.02	778
29	0.005	1.60	0.125	30.8	5.00 ± 0.10	2464
24	0.005	2.15	0.50	90.3	34.2 ± 1.0	12350
24	0.005	2.15	0.50	89.0	35.3 ± 1.0	12640
24	0.005	1.80	0.50	86.2	17.1 ± 0.9	5900
24	0.005	1.60	0.50	85.0	8.4 ± 0.4	2840
24	0.005	0.95	0.50	59.0	0.8 ± 0.04	190
24	0.005	0.65	0.50	28.0	0.11 ± 0.02	12.3
24	0.005	1.70	0.50	82.4	6.2 ± 0.40	2060
24	0.005	1.00	0.50	61.5	0.60 ± 0.04	153
24	0.005	0.55	0.50	24.1	0.050 ± 0.002	4.8
24	0.004	1.72	0.500	93.7	9.6 ± 0.8	3600
24	0.004	1.76	0.250	71.2	7.7 ± 0.5	4188
24	0.004	1.82	0.125	47.5	8.0 ± 0.3	6080
24	0.004	1.86	0.063	31.2	7.6 ± 0.6	7524
24	0.004	1.90	0.31	21.2	6.5 ± 0.4	7240

*Optical path in stopped-flow cell: 2 cm.

TABLE II. Kinetic Data for the Reaction Ti(III) and Pyrunic Acid Obtained by Conventional Spectrophotometry (Low pH Region).

Temp. °C	$\{Ti^{3+}\}_o$ M	$\{H^+\}$	$\{PYR\}_o$	ϵ M^{-1} cm^{-1}	10^2 $k_{obs}^{(3)}$ s^{-1} M^{-2}
7.5	0.0132	1.8	0.214	4.8	1.17
25	0.0132	1.8	0.214	4.8	6.28
35	0.0132	1.8	0.214	4.8	13.46
42.5	0.0132	1.8	0.214	4.8	26.47
14	0.0142	0.8	0.107	4.6	8.3
24	0.0142	0.8	0.107	4.6	19
36	0.0142	0.8	0.107	4.6	56
46	0.0142	0.8	0.107	4.6	120
14	0.0142	1.4	0.107	4.6	2.80
24	0.0142	1.4	0.107	4.6	6.40
36	0.0142	1.4	0.107	4.6	17.10
46	0.0142	1.4	0.107	4.6	36.50
24	0.005	0.22	1.00	43.4	2.050
24	0.005	0.22	0.50	30.2	1910
24	0.005	0.22	0.25	16.1	1710
24	0.005	0.22	0.12	8.5	2140
24	0.020	0.65	1.00	23.5	121
24	0.020	1.05	1.00	14.6	37
24	0.020	1.36	1.00	10.3	12.4
24	0.020	1.76	1.00	8.5	6.8
24	0.020	1.92	1.00	7.2	5.3
24	0.020	2.45	1.00	6.6	2.9
24	0.20	0.57	1.00	24.3	177
24	0.020	0.57	0.80	20.3	222
24	0.020	0.57	0.60	13.1	174
24	0.020	0.57	0.40	8.9	177
24	0.020	0.57	0.20	5.2	182
24	0.020	0.57	0.10	4.6	187

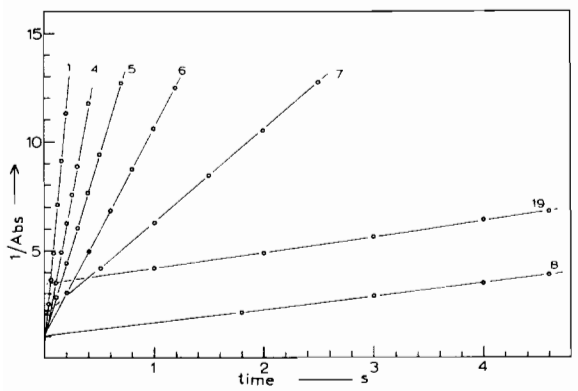

Fig. 3. Typical second order plots for the redox reaction between Ti^{3+} and pyruvic acid. The kinetic data for these plots were obtained by the stopped-flow instrument. The numbers of these lines correspond to the runs as they appear on Table II.

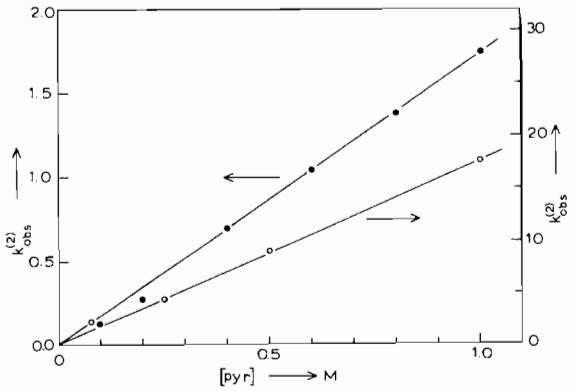

Fig. 4. Plots of $k_{obs}^{(2)}$ *vs.* pyruvic acid concentration at 24 °C. Full circles correspond to pH = 0.25. Open circles correspond to pH = 0.62.

centration of hydrogen ion, while the rate of reduction by V_{aq}^{2+} was found [5] to be acid independent. Figure 5 is a plot of log $k_{obs}^{(3)}$ *vs.* log(1/{H$^+$}). For a change in {H$^+$} by two-and-a-half orders of magnitude the observed rate constant changes by *ca.* five orders of magnitude.

The observed activation parameters, E_{obs} and A_{obs}, at various hydrogen ion concentrations, are included in Table III.

These uncorrected parameters were estimated assuming that hydrogen ion concentration and the ratio keto/hydro of pyruvic acid do not change with temperature. This, however, is only approximately true at high acidities. At low acidities they must be corrected.

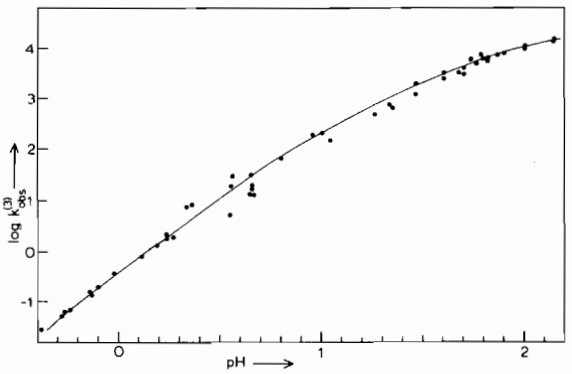

Fig. 5. Dependence of $k_{obs}^{(3)}$ on hydrogen ion concentration. Forty nine values of this rate constant at different pH values are shown on this graph. All these values are normalized at 24 °C.

TABLE III. Activation Parameters for the Ti^{III}–pyr Reaction at Various Hydrogen Ion Concentrations.

$\{H^+\}$, (*M*)	E_{obs} (kcal mol^{-1})	A_{obs}	E_{cor}
1.8	15.5 ± 0.5	10.2 ± 0.5	15.5 ± 0.5
1.4	14.9 ± 0.4	9.7 ± 0.3	14.9 ± 0.4
0.8	15.6 ± 0.4	10.7 ± 0.2	15.6 ± 0.4
pH = 2.07[a]	9.5 ± 0.3	6.98 ± 0.3	14.5 ± 0.5

[a]At 22 °C. See text.

The corrections for the change of $\{H^+\}$ with temperature were made on the basis of the empirical curve in Fig. 6. The change in pH affects in turn the ratio of the active keto-form of pyruvic acid over the inactive hydro-form. Corrections for this change were based on the data reported by Pocker *et al.* [7]. Within experimental error, the corrected value for the activation energy (E_{corr} = 14.5 ± 0.5 kcal mol^{-1}) at pH 2 is the same as those obtained at higher acidities (Table III).

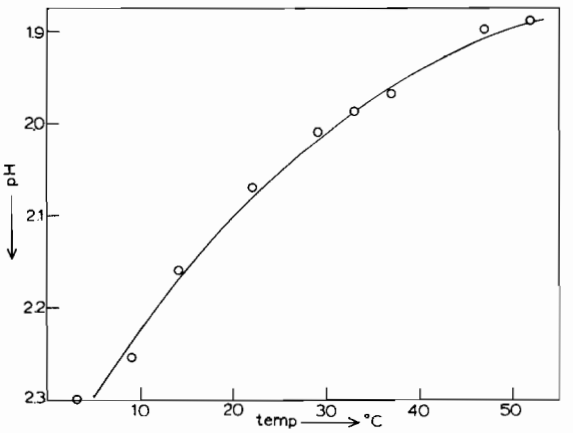

Fig. 6. Dependence of pH of the pyrH/pyr^- buffer solution upon temperature. [pyrH] = 0.303 *M* and [pyr^-] = 0.197 *M*.

Discussion

Only one path is indicated by the kinetic results, throughout the hydrogen ion concentration range investigated. Activation energies at various acidities are the same. The overall slope of the log $k_{obs}^{(3)}$ *vs.* $-\log\{H^+\}$ plot is two (Fig. 5). The deviation from linearity of this plot is not significant, which can be attributed to the following factors. Firstly, the rate constants in this figure were estimated using the total concentration of pyruvic acid, but only the keto-form is reactive and the ratio keto/hydro depends on pH [7]. At pH values higher than *ca.* 3.5 most pyruvate (*ca.* 95%) is in the keto-form, whereas at pH values lower than *ca.* 1 only *ca.* 40% is in this form. Thus, in order to obtain the real rate constants at high acidities, we must divide by 0.4, and this will bring up the points on the left in Fig. 5, and improve linearity.

A second factor contributing to the non-linearity of the log $k_{obs}^{(3)}$ *vs.* $\log\{H^+\}$ plot must be the fact that pH values larger than *ca.* 0.3 were measured by a pH-meter, whereas for pH < 0.3 the hydrogen ion concentration was estimated from the acid added.

Finally, Ti^{III} itself and the product of its oxidation, Ti^{IV}, are expected to affect the keto/hydro ratio, because of their acidic character and of some fractionation resulting from complexation.

The rate law corresponding to the dominating path for the redox step is:

$$\text{Rate} = k\frac{\{Ti^{III}\}^2\{\text{pyr-keto}\}}{\{H^+\}^2}$$

and it is remarkable that even at high acidities this path is the only measurable one. The fast complex formation on the other hand makes it very likely that the composition of the activated complex indicated by the rate law corresponds to a dinuclear, pyruvate-bridged, Ti^{III} precursor complex.

The necessity for removing two protons is related to the driving force of the reaction. Pyruvate is more readily reduced than pyruvic acid and hydrolyzed Ti^{III} is more readily oxidized. At this stage it is not clear where exactly the protons are removed from, but it seems reasonable to speculate that one is removed from the carboxylic group in order to facilitate complexation, and the other from a coordinated water molecule. The dependence of the average absorptivity on both {pyr} and $\{H^+\}$ as well as the stoichiometry, the products obtained and the rate law are all consistent with a doubly bridged structure for the precursor complex, and a mechanism of the form:

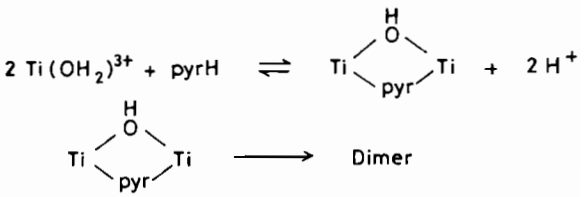

It should be pointed out, however, that even though the two electron donors interact simultaneously with a pyruvate, only one electron is transfered, presumably because the two Ti^{III} are bound to non-neighboring sites of the organic moiety.

In a previous study [8] we presented evidence for the formation of an 1:1 adduct between a reducing metal ion and a carbon–carbon double bond, and showed that this complex undergoes further reactions such as attack by a second reducing metal ion, homolytic cleavage, and free radical formation. For the Ti^{III} pyruvate system the dominating path is ion-radical formation, which can be regarded as a special case of free radical formation. A possible scheme would involve the reaction:

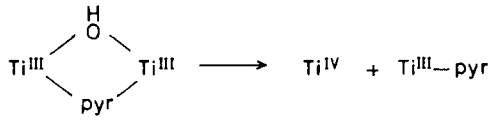

followed by a coupling, similar to the pinacolic coupling induced by organometallic compounds of early transition elements [1].

On theoretical grounds, one can argue that at least the first interaction between Ti^{III} and the C=O double bond involves a Dewar–Chatt–Duncanson [9] type of complex. In contrast to chromium(II), titanium(III) and vanadium(II) are expected to coordinate symmetrically or nearly symmetrically. In this way the overlap is maximized. A large number of analogous structures are known. The increased absorptivities of the complexes of Ti^{III} (Figs. 1 and 2) and of V^{II} with unsaturated systems [5, 10] can be attributed to the charge transfer inherent in the Dewar–Chatt–Duncanson model. In fact, in the case of V^{II} + maleic acid there is direct evidence for the activation of the double bond, namely isomerization to fumaric acid and exchange of the hydrogens bound to the double-bond carbons with the solvent. Also, formation constants for V^{II}–maleic acid complexes are [10] one or two orders of magnitude larger than the corresponding constants for other (non-donor) bivalent metal ions.

From the energy level diagram of the η^2 model (Fig. 7) we see that the second electron can enter a partly-occupied metal-ion-centered orbital: there is a contribution to activation from electron repulsion. Such a contribution is absent if the electron enters the empty antibonding $\pi^* - \lambda b_2$, but this orbital lies higher. Entrance into the unaffected metal orbitals does not lead directly to reduction. In any case, an increased barrier is expected for a two-electron change. This must be one of the reasons then that reductions by Ti^{III} or V^{II} give one-electron reduction products (dimers), in contrast to Cr^{II} and Eu^{II}, where η^1 models apply [5, 8] and double-bond hydrogenations are observed.

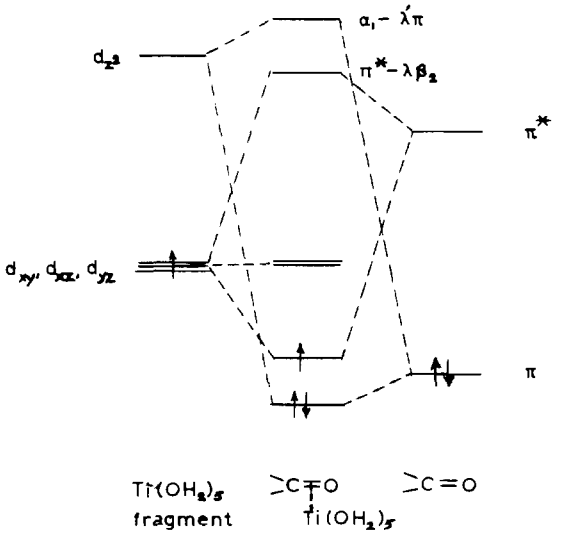

Fig. 7. Qualitative energy level diagram for the Dewar–Chatt–Duncanson model of a titanium(III)–carbonyl complex.

In lieu of a conclusion we may note that the two-electron and one-electron paths identified for the carbonate-like pyruvic acid and/or for pyruvate involve η^1 and η^2 intermediates, respectively. For carbonate itself these paths would correspond to formate and oxalate formation.

Acknowledgements

The authors thank Mr. S. Loukas for the NMR identification of products, and Mrs. E. Meidani and Mrs. M. Katsarou for technical assistance.

References

1 G. Fachinetti, C. Floriani, A. Chiesi-Villa and C. Guastini, *J. Am. Chem. Soc., 101*, 1767 (1979); G. Fachinetti, C. Floriani and P. F. Zanazzi, *ibid., 100*, 7405 (1978); M. Pasquali, S. Gambarotta, C. Floriani and A. Chiesi-Villa, *Inorg. Chem., 20*, 165 (1981); M. Pasquali, C. Floriani, A. Chiesi-Villa and C. Guastini, *ibid., 20*, 349 (1981); S. Gambarotta, M. Pasquali, C. Floriani and A. Chiesi-Villa, *ibid., 20*, 1173 (1981).
2 S. D. Ittel, *J. Organometal. Chem., 137*, 223 (1977); *Inorg. Chem., 16*, 2589 (1977); J. Burges, J. G. Chambers, D. A. Clarke, R. D. Kemmitt, *J. Chem. Soc., Dalton Trans.*, 1906 (1977); D. A. Clarke, M. M. Hunt, J. C. Huffman, J. K. Kochi, *Inorg. Chem., 18*, 2311 (1979); J. Browing, H. D. Empsall, M. Green, F. G. A. Stone, *J. Chem. Soc., Dalton Trans.*, 381 (1973).
3 J. B. Conant and H. B. Cutter, *J. Am. Chem. Soc., 48*, 1016 (1926).
4 A. Petrou, E. Vrachnou-Astra and D. Katakis, *Inorg. Chim. Acta, 39*, 161 (1980).
5 J. Konstantatos, E. Vrachnou-Astra, N. Katsaros and D. Katakis, *Inorg. Chem., 21*, 122 (1982); *J. Am. Chem. Soc., 102*, 3035 (1980); *ibid., 100*, 3128 (1978).

6 G. A. K. Thompson and A. G. Sykes, *Inorg. Chem., 15*, 638 (1976).
7 Y. Pocker, J. E. Meany, B. J. Nist and C. Zadorojny, *J. Phys. Chem., 73*, 2879 (1969).
8 Submitted for publication.
9 M. J. B. Dewar, *Bull. Soc. Chim. Fr., 48*, 112 (1951); J. Chatt and L. A. Duncanson, *J. Chem. Soc.*, 2939 (1953).
10 E. Vrachnou-Astra, P. Sakellaridis and D. Katakis, *J. Am. Chem. Soc., 92*, 811 (1970); E. Vrachnou-Astra, P. Sakellaridis and D. Katakis, *ibid., 92*, 3936 (1970); E. Vrachnou-Astra and D. Katakis, *ibid., 89*, 6772 (1967).